

DEVELOPMENT OF AIR POLLUTANTS DISPERSION ALGORITHM IN  
URBAN INDUSTRIAL PARK FOR AIR POLLUTION SIMULATION

UBAIDULLAH BIN SELAMAT

A thesis submitted in fulfilment of the  
requirements for the award of the degree of  
Doctor of Philosophy

School of Mechanical Engineering  
Faculty of Engineering  
Universiti Teknologi Malaysia

OCTOBER 2019

## **DEDICATION**

This thesis is dedicated to Umi and Abi, Mak and Ayah, and all my family members who taught me that the best kind of knowledge to have is that which is learned for its own sake. It is also dedicated to my beloved wife and children, Nur Amira, Maryam Hannah, Muhammad Yusuf Faris who taught me that even the largest task can be accomplished if it is done one step at a time.

## ACKNOWLEDGEMENT

In preparing this thesis, I was in contact with many people, researchers, academicians, and practitioners. They have contributed towards my understanding and thoughts. In particular, I wish to express my sincere appreciation to my main thesis supervisor, Dr. Muhamad Hasbullah Padzillah, for encouragement, guidance, critics and friendship. I am also thankful to my co-supervisor Associate Professor Dr. Kahar Osman for his thorough guidance, advices and motivation. Without their continued support and interest, this thesis would not have been the same as presented here.

I am also indebted to Universiti Teknologi Malaysia (UTM), Majlis Amanah Rakyat (MARA) and Kementerian Pendidikan Tinggi (KPT) for funding my Ph.D study. Assoc. Prof. Takahisa Yamamoto from Gifu National College of Technology, Japan also deserve special thanks for his assistance in numerical and turbulence implementations.

My fellow Computational Fluid Mechanics (CFM) laboratory members should also be recognised for their support especially to Hazmil, Zamani, Ikhwan, Hakim, Rashidi and others. My sincere appreciation also extends to all my colleagues and others who have provided assistance at various occasions. Their views and tips are useful indeed. Unfortunately, it is not possible to list all of them in this limited space.

I am truly grateful to all my family members. A very special thanks to my lovely and beloved wife, Nur Amira for continuous support and countless sacrifices through hardship in all these years. This thesis would not have been completed without her being on my side.

## ABSTRACT

Environmental Impact Assessment analysis is generally restricted to neighbourhood scale air pollution simulation using the Gaussian Plume model (GPM). This approach expected to enhance the resolution of ground level concentration in the conventional GPM based software up to building scale by using Computational Fluid Dynamics (CFD) model alongside the GPM. The aim of this study was to develop an air pollution prediction algorithm for air pollutants release from industrial stacks. It was used to estimate, simulate and control air pollution in urban industrial park using integrated GPM and CFD model. The GPM was used for regional air pollutant level prediction to find high pollutant concentration zones. Whereas, CFD model was used for detailed simulation on respective polluted areas. In order to achieve this, a building detection algorithm from satellite image based on building footprint detection and height estimation from shadow thickness has been proposed to reduce pre-processing effort of the present CFD solver. The present CFD algorithm were based on Fractional Step Method for efficient steady state solver and Prandtl Mixing Length turbulence model for low cost turbulence calculation. The accuracy of the CFD algorithm has been tested and verified against benchmark problems (less than 3% error for lid-driven cavity problem, less than 8% for flow over isolated cube). It was discovered that CFD algorithm developed in this study is sufficiently accurate as other wind flow models with slight over prediction in wind speed by 1.04 m/s (15.6% are below 10% error) and able to predict the wind direction correctly within 60° angle (37.5% are within 15° angle) compared to measurement data. Air pollutant release from major stacks in Pasir Gudang Industrial Park was studied using GPM and high NO<sub>2</sub> concentration zone (1800 µg/m<sup>3</sup>) was found in Taman Air Biru. Results suggest that 24-hour averaged SO<sub>2</sub> and PM<sub>10</sub> maximum ground level concentration are well within Ambient Air Quality Standard (AAQS) limits with 8.9 µg/m<sup>3</sup> (8.4%) and 11.4 µg/m<sup>3</sup> (7.6%) respectively. Meanwhile, 24-hour averaged NO<sub>2</sub> concentration exceed AAQS limit with 270.3 µg/m<sup>3</sup> (360%). The detailed CFD simulation of wind distribution and pollutant dispersion process within the area was presented. Present CFD model (1800 µg/m<sup>3</sup>) over predicted 1-hour averaged NO<sub>2</sub> ground concentrations by a factor of 3 compared to the present GPM (700 µg/m<sup>3</sup>) but it provides more information on wind distribution as well as pollutant dispersion process. A new atmospheric dispersion solver has been developed that is able to simulate pollutant dispersion on both regional scale using GPM and building scale using CFD model.

## ABSTRAK

Analisis Penilaian Kesan Alam Sekitar umumnya terhadap kepada skala kejuranan bagi simulasi bahan pencemar udara menggunakan model Gaussian Plume (GPM). Kaedah ini menambahbaik resolusi simulasi kepekatan bahan pencemar atas tanah dalam perisian konvensional GPM kepada skala bangunan dengan menggabungkannya bersama model Dinamik Bendalir Berkomputer (CFD). Kajian ini bertujuan untuk membangunkan algoritma ramalan pencemaran udara bagi pelepasan bahan pencemar daripada cerobong asap industri. Ia digunakan untuk meramal, mensimulasi dan mengawal pencemaran udara di kawasan perindustrian bandar dengan menggunakan GPM dan model CFD yang disatukan dalam satu algoritma. GPM digunakan untuk meramal tahap pencemaran udara secara kasar bagi mencari kawasan berkepekatan tinggi. Model CFD pula digunakan untuk simulasi terperinci di kawasan berkepekatan tinggi tersebut. Algoritma pengesanan bangunan dari imej satelit menggunakan teknik pengesanan tapak bangunan dan anggaran ketinggian bangunan berdasarkan ketebalan bayang telah dibangunkan untuk meringkaskan pra-pemprosesan model CFD. Dalam tesis ini, algoritma CFD menggunakan kaedah *fractional step* untuk penyelesaian secara efisien dan model pergolakan *Prandtl Mixing Length* untuk pengiraan yang pantas. Ketepatan algoritma ini telah diuji dan disahkan menggunakan data eksperimen piawai dan kajian eksperimen secara berperingkat (kurang 3% untuk kaviti, kurang 8% untuk pergerakan udara merentasi kiub). Hasil kajian menunjukkan algoritma CFD yang dibangunkan adalah cukup tepat kerana model pergerakan angin meramal sebanyak 1.04 m/s (15.6% mempunyai sisihan kurang 10%) lebih tinggi daripada dapatan eksperimen dan dapat meramalkan arah angin dengan betul dalam lingkungan sudut 60° (37.5% mempunyai sisihan kurang 15°) berbanding dengan data piawai. Pencemaran udara dari cerobong asap utama di Taman Perindustrian Pasir Gudang telah dikaji menggunakan GPM dan zon kepekatan NO<sub>2</sub> yang tinggi terdapat di Taman Air Biru. Keputusan mencadangkan bahawa kepekatan purata 24-jam SO<sub>2</sub> dan PM<sub>10</sub> adalah di bawah had kualiti udara (AAQS) iaitu sebanyak 8.9 µg/m<sup>3</sup> (8.4%) dan 11.4 µg/m<sup>3</sup> (7.6%). Sementara itu, kepekatan purata 24-jam NO<sub>2</sub> melebihi had AAQS sebanyak 270.3 µg/m<sup>3</sup> (360%). Simulasi CFD yang terperinci terhadap pergerakan angin dan proses penyebaran pencemar di kawasan ini telah dibentangkan. Model CFD dalam kajian ini (1800 µg/m<sup>3</sup>) terlebih anggar kepekatan purata 1-jam NO<sub>2</sub> dengan faktor 3 berbanding GPM (700 µg/m<sup>3</sup>) tetapi ia mempunyai data yang lebih lengkap mengenai taburan angin dan juga proses pergerakan bahan pencemar udara. Algoritma penyebaran bahan pencemar udara yang baru telah dibangunkan bagi mensimulasikan penyebaran bahan pencemar udara pada kedua-dua skala serantau menggunakan GPM dan skala bangunan menggunakan model CFD.

## TABLE OF CONTENTS

	<b>TITLE</b>	<b>PAGE</b>
	<b>DECLARATION</b>	<b>ii</b>
	<b>DEDICATION</b>	<b>iii</b>
	<b>ACKNOWLEDGEMENT</b>	<b>iv</b>
	<b>ABSTRACT</b>	<b>v</b>
	<b>ABSTRAK</b>	<b>vi</b>
	<b>TABLE OF CONTENTS</b>	<b>vii</b>
	<b>LIST OF TABLES</b>	<b>xi</b>
	<b>LIST OF FIGURES</b>	<b>xiii</b>
	<b>LIST OF ABBREVIATIONS</b>	<b>xix</b>
	<b>LIST OF SYMBOLS</b>	<b>xxi</b>
	<b>LIST OF APPENDICES</b>	<b>xxiii</b>
<b>CHAPTER 1</b>	<b>INTRODUCTION</b>	<b>1</b>
1.1	Research Background	1
1.2	Problem Statement	5
1.3	Research Objectives	6
1.4	Significance of Study	7
1.5	Scope of Study	7
<b>CHAPTER 2</b>	<b>LITERATURE REVIEW</b>	<b>9</b>
2.1	Overview of Air Pollution Models	9
2.1.1	Gaussian-type models	9
2.1.2	Langrangian-type models	11
2.1.3	Eulerian-type models	12
2.1.4	Models Integration	14
2.2	Computational Fluid Dynamics in Urban Air Pollutant Simulation	15
2.2.1	Effects of Building Dimension and Configuration	16

2.2.2	Effects of Trees and Vehicles	17
2.2.3	CFD on Urban Industrial Stacks	20
2.2.4	Simulation Scale	22
2.2.5	CFD on Urban Design	23
2.3	Geospatial Data in Air Pollution Software	24
2.3.1	Geo Information System (GIS)	25
2.3.2	Satellite Image	28
2.4	Integration of Spatial Data and CFD solver	29
2.4.1	Limitations of Existing Commercial Software	32
2.4.2	Satellite Image Building Extractor	34
2.5	Air Pollution in Pasir Gudang	37
2.5.1	Field Measurements and Air Pollutants Sampling	38
2.5.2	Air Pollutant Modelling	39
2.5.3	Climate and Wind Data	39
2.6	Summary of Literature Review	40
<b>CHAPTER 3</b>	<b>METHODOLOGY</b>	<b>45</b>
3.1	Introduction	45
3.2	Gaussian Plume Model	45
3.3	Computational Fluid Dynamics Model	47
3.3.1	Governing Equations	47
3.3.2	Reynolds Averaged Navier-Stokes (RANS) Equation	48
3.3.3	Turbulence Model (Prandtl Mixing Length)	49
3.3.4	Numerical Implementation	51
3.3.4.1	Fractional Step Method	51
3.3.4.2	Air Pollutant Dispersion	53
3.3.4.3	Boundary Conditions and Near Wall Treatment	54
3.3.5	Grid and Meshing	57
3.4	Satellite Image Building Generator	59
3.4.1	Building Footprint Detection	59

3.4.1.1	Color Band Thresholding	60
3.4.1.2	Building Footprint Segmentation	62
3.4.1.3	Vegetation and Shadow Removal	63
3.4.1.4	Building Delineation	63
3.4.2	Building Height Estimation from Shadow Thickness	64
3.5	Algorithms Flowchart	66
3.6	Algorithm Validation and Performance Evaluation	71
3.7	Pasir Gudang Air Pollutant Prediction and Simulation	77
<b>CHAPTER 4</b>	<b>RESULTS AND DISCUSSION</b>	<b>81</b>
4.1	Introduction	81
4.2	Case Study I – Algorithm Validation and Performance Evaluation	81
4.2.1	Gaussian Plume Algorithm	81
4.2.2	Satellite Image Building Generator	87
4.2.2.1	Building Footprint Detection Algorithm	87
4.2.2.2	Height Estimation Algorithm	94
4.2.2.3	Integration of Building Footprint Detection and Height Estimation	98
4.2.3	CFD Solver	103
4.2.3.1	Lid Driven Cavity Benchmark Problem	103
4.2.3.2	Comparison with Flow over Isolated Cube Benchmark Problem	108
4.2.3.3	Comparison with Joint Urban 2003 Field Experiment	113
4.3	Case Study II – Pasir Gudang Air Pollutant Prediction and Simulation	122
4.3.1	Regional Scale Estimation using Gaussian Plume model	123
4.3.1.1	Comparison with Atmospheric Dispersion Model	123
4.3.1.2	Comparison with Field Measurement	132



4.3.2	Building Scale Simulation using CFD Model at High Concentration Zone	135
4.3.2.1	Predicted High Concentration Zone	138
4.3.2.2	Urban Structures Generation Using Present Satellite Image Building Extractor	139
4.3.2.3	Wind Flow Distribution	140
4.3.2.4	Pollutant Dispersion and Ground Concentration	144
<b>CHAPTER 5</b>	<b>CONCLUSION AND RECOMMENDATIONS</b>	<b>151</b>
5.1	Research Conclusion	151
5.2	Contributions to Knowledge	153
5.3	Future Works	153
	<b>REFERENCES</b>	<b>155</b>
	<b>LIST OF PUBLICATIONS</b>	<b>167</b>
<b>APPENDIX A</b>	<b>Detailed Gaussian Plume Model (IMMDADS Software)</b>	<b>169</b>
<b>APPENDIX B</b>	<b>Publications</b>	<b>177</b>



Table 4. 14	Comparison of Ground-Level Concentration	131
Table 4. 15	PM <sub>10</sub> concentration of 4 residential areas (Rozana <i>et al.</i> , 2009) and present study (24-hour averaged)	133
Table 4. 16	Measured and predicted GLC for all pollutants in Pasir Gudang monitoring station	134

## LIST OF FIGURES

FIGURE NO.	TITLE	PAGE
Figure 1. 1	(a) Location of Pasir Gudang Industrial Park (b) Neighbourhood scale ( $10^4$ m or 10 km x10 km using Gaussian Plume model) (c) Building scale ( $10^3$ m or 1 km x 1 km using CFD model) (Google Maps, 2019).	4
Figure 2. 1	Conical plume assumption used in Gaussian Plume model (Beychok, 2005).	10
Figure 2. 2	Ground concentration output from Gaussian models (P1, P2, P3 and P4 as the source) (Tartakovsky et. al., 2016)	11
Figure 2. 3	Puff particles in Lagrangian Particle Tracking models (Szabo, 2016)	11
Figure 2. 4	Cumulated number of puffs converted as ground concentration in Lagrangian models (Tang et. al., 2018)	12
Figure 2. 5	Wind varies locally and disperse within buildings in CFD model (Boppana et. al., 2019)	13
Figure 2. 6	Calculated concentration contours at 1.6 m compared with measured concentration contour at 1 ppm for field scale scenario (Antonioni <i>et al.</i> , 2012).	14
Figure 2. 7	Velocity magnitude contours and vectors of multiple urban street canyons with buildings (black) (a) normal buildings (b) buildings with ventilation on ground floor (Chew and Norford, 2018).	16
Figure 2. 8	Recirculation region (dark colour) that hinder pollutant removal (Bijad, 2016)	17
Figure 2. 9	Schematic of vehicle movement study (a) Schematics of vehicle passing urban street canyon (b) Common pedestrian and vehicle lanes (Li <i>et al.</i> , 2017)	18
Figure 2. 10	Comparison of CFD and Gaussian model (a) Ground concentration (CFD) (b) Ground concentration (Gaussian) (c) CO concentration for Gaussian and CFD (d) NO concentration for Gaussian and CFD (Bady, 2017)	20
Figure 2. 11	Detailed simulation results of Carbon concentration (ppm) (Toja-Silva <i>et al.</i> , 2017)	21

Figure 2. 12	Multiple scale urban air pollutant problems (Cui <i>et al.</i> , 2016)	22
Figure 2. 13	Multi-layer of information in geospatial database (US GAO, 2017).	24
Figure 2. 14	Walking activities distribution in Glasgow, UK (Sun <i>et al.</i> , 2017)	26
Figure 2. 15	Spatial distribution of NO <sub>x</sub> in roundabouts (Sanchez <i>et al.</i> , 2017)	27
Figure 2. 16	Projected simulation results and damage distribution onto satellite image (Pontiggia <i>et al.</i> , 2011)	29
Figure 2. 17	Footprints traced using AC3D software (Houda <i>et al.</i> , 2017)	30
Figure 2. 18	Generated discrete domain of Tokyo city. The isosurface (yellow) corresponds to pollutant release (Toja-Silva <i>et al.</i> , 2018a)	30
Figure 2. 19	CFD solver novel feature available in present algorithm (a) (Google Maps, 2019) (b) (Gowardhan <i>et al.</i> , 2011) (c) (Dominik B., 2017)	32
Figure 2. 20	Features detection of buildings and street networks (Grinias <i>et al.</i> , 2016)	35
Figure 2. 21	Height estimation from SAR image (Wang <i>et al.</i> , 2018)	36
Figure 3. 1	2D flow over square-shaped building	54
Figure 3. 2	Staggered grid used in present study	58
Figure 3. 3	Sample satellite image (left) and resulting colour band thresholding process (right)	62
Figure 3. 4	Output of centroid identification algorithm	62
Figure 3. 5	Output of building delineation algorithm	64
Figure 3. 6	Shadow regions after shadow detection algorithm	64
Figure 3. 7	Pixel counting direction (red) for height estimation from shadow thickness (bottom left building)	65
Figure 3. 8	Algorithm flowcharts (a) Building Detection (b) Height Estimation	67
Figure 3. 9	Algorithm flowcharts (a) Building Generator (b) Fluid Solver Pre-processing.	68
Figure 3. 10	Flowcharts of Solver Time Iteration	69

Figure 3. 11	Flowcharts of Pollutant Transport and Post processing	70
Figure 3. 12	Boundary conditions for lid-driven cavity flow (Ghia et. al., 1982)	74
Figure 3. 13	Satellite image of Oklahoma City (Google Maps, 2019)	75
Figure 3. 14	Building footprints of Oklahoma City (Gowardhan et. al., 2011)	76
Figure 3. 15	Wind rose of Senai Monitoring Station for year 2009	78
Figure 4. 1	Comparison of maximum GLC for ISC and IMMDADS (present) for CASE 1	84
Figure 4. 2	Comparison of maximum GLC for ISC and IMMDADS (present) for CASE 2	84
Figure 4. 3	Comparison of maximum GLC for ISC and IMMDADS (present) for CASE 3	85
Figure 4. 4	Comparison of maximum GLC for ISC and IMMDADS (present) for CASE 4	85
Figure 4. 5	Building detection output of (a) Tested satellite image (b) (Benedek et al., 2015) (c) (Sumer and Turker, 2013) and (d) present algorithm	88
Figure 4. 6	Comparison chart of performance parameters	90
Figure 4. 7	Resulting images from algorithm (a) Satellite image (b) Building footprints and centroids (c) Building Edges (d) Building delineation (e) Finalized footprint without delineation	91
Figure 4. 8	a) Original image and (b) resulting detected buildings in NIT, Japan	93
Figure 4. 9	Test image for height estimation algorithm (Manno-Kovacs and Sziranyi, 2015)	94
Figure 4. 10	(a) Buildings centroid and (b) detected shadow. Red boxes show Segment 17-22)	94
Figure 4. 11	Detected shadow region (Image 1) (a) Satellite image (b) Gregoris et. al. (2016) (c) Present algorithm	96
Figure 4. 12	Detected shadow region (Image 2) (a) Satellite image (b) Gregoris et. al. (2016) (c) Present algorithm	96
Figure 4. 13	Comparison Chart for calculated height between Gregoris et. al., 2016 and present study (Segment 1-7 for Image 1 and Segment 1-2 for Image 2).	97

Figure 4. 14	Satellite image used in Feng Qi et. al. (2016) (a) Zone A (b) Zone B (c) Zone C	98
Figure 4. 15	Images acquired used in present study (a) Zone A (b) Zone B (c) Zone C	99
Figure 4. 16	Detected building foot prints for Zone A (a) and Zone B (b)	99
Figure 4. 17	Shadow detection in present algorithm (a) Zone A (b) Zone B (c) Zone C	100
Figure 4. 18	Building detection with height estimation (a) Satellite image (b) Footprints and centroids (c) Shadow estimation	101
Figure 4. 19	Comparison charts of calculated height of Feng Qi et. al., 2016 and present study	102
Figure 4. 20	Velocity vectors (a) and streamlines (b) of $Re = 100$ with $30 \times 30$ mesh (present study)	104
Figure 4. 21	Velocity vectors (a) and streamlines (b) of $Re = 400$ with $60 \times 60$ mesh (present study)	104
Figure 4. 22	Velocity vectors (a) and streamlines (b) of $Re = 1000$ with $90 \times 90$ mesh (present study)	104
Figure 4. 23	Horizontal U-velocity across geometric centre, $Re = 100, 400, 1000$ between Ghia (1982) and present study	107
Figure 4. 24	Vertical V-velocity across geometric centre, $Re = 100, 400, 1000$ between Ghia (1982) and present study	107
Figure 4. 25	Velocity vectors of wind tunnel data (black) and CFD results by Gowardhan et. al. (2011) (grey). (Side view)	108
Figure 4. 26	Velocity vectors from present algorithm (Side view)	109
Figure 4. 27	Velocity vectors of wind tunnel data (black) and CFD results by Gowardhan et. al. (2011) (grey). (Top view)	110
Figure 4. 28	Velocity vectors of present algorithm. (Top view)	110
Figure 4. 29	Present algorithm profiles (line) overlapped with wind tunnel data (dot)	112
Figure 4. 30	Contours of $u'w'$ in the x-z plane for Gowardhan et. al. (2011)	112
Figure 4. 31	Contours of $u'w'$ in the x-z plane for present study	113

Figure 4. 32	Detected building footprints (a) and shadows (b) using present algorithm	114
Figure 4. 33	Buildings isosurface generated in present algorithm	114
Figure 4. 34	Velocity vectors generated using present algorithm (buildings are rotated inside whereas boundary is fixed in present algorithm)	115
Figure 4. 35	Velocity vectors at centre region (red box) (a) field measurement (black arrow) and Gowardhan (2011) (grey arrow) (b) present algorithm	116
Figure 4. 36	Horizontal velocity vectors overlapped with velocity magnitudes (a) Gowardhan et. al. (2011) (b) present algorithm	118
Figure 4. 37	Vertical velocity vectors overlapped with velocity magnitudes (a) Gowardhan et. al. (2011) (b) present algorithm	119
Figure 4. 38	Computed and observed wind direction of present study	121
Figure 4. 39	Computed and observed wind speed of present study	122
Figure 4. 40	24-hour SO <sub>2</sub> GLC distribution (a) maximum location (red) (b) areas exceeded allowable limits (90 µg/m <sup>3</sup> )	124
Figure 4. 41	Annual SO <sub>2</sub> GLC distribution (a) maximum location (red) (b) areas exceeded allowable limits (50 µg/m <sup>3</sup> )	125
Figure 4. 42	24-hour NO <sub>2</sub> GLC distribution (a) maximum location (red) (b) areas exceeded allowable limits (75 µg/m <sup>3</sup> )	126
Figure 4. 43	Annual NO <sub>2</sub> GLC distribution (a) maximum location (red) (b) areas exceeded allowable limits (40 µg/m <sup>3</sup> )	127
Figure 4. 44	24-hour PM <sub>10</sub> GLC distribution (a) maximum location (red) (b) areas exceeded allowable limits (150 µg/m <sup>3</sup> )	128
Figure 4. 45	Annual PM <sub>10</sub> GLC distribution (a) maximum location (red) (b) areas exceeded allowable limits (50 µg/m <sup>3</sup> )	129
Figure 4. 46	24-hour PM <sub>10</sub> concentration.	132
Figure 4. 47	1-hour ground concentration of NO <sub>2</sub> for northwest to southeast wind (1.5 m/s) (a) and regions exceeded limits (b) using present algorithm	136
Figure 4. 48	1-hour ground concentration of NO <sub>2</sub> for south to north wind (1.5 m/s) (a) and regions exceeded limits (b) using present algorithm	137



Figure 4. 49	Predicted high NO <sub>2</sub> region in Taman Air Biru (red circle) located at northern Stack 35 (red dot)	138
Figure 4. 50	Enlarged view (a) and detected footprints (b) using present algorithm	139
Figure 4. 51	Mesh generated by present algorithm of respective area after height estimation process	140
Figure 4. 52	Velocity magnitudes overlapped with horizontal velocity at 6.5 m height (A - B Plane is the plume cross section)	141
Figure 4. 53	Horizontal velocity magnitudes at plume cross section (A-B Plane)	142
Figure 4. 54	Velocity streamlines at 6.5 m height	143
Figure 4. 55	Turbulent eddy viscosity, $\nu_t$ at 6.5 m height	144
Figure 4. 56	1-hour concentration of NO <sub>2</sub> at ground-level at 6.5 m height	145
Figure 4. 57	1-hour concentration of NO <sub>2</sub> at plume cross section (A-B Plane)	146
Figure 4. 58	NO <sub>2</sub> GLC for first 10 minutes at 6.5 m height (a) 2 minutes (b) 4 minutes (c) 6 minutes (d) 8 minutes (e) 10 minutes	147
Figure 4. 59	NO <sub>2</sub> GLC for first 10 minutes at plume cross section (a) 2 minutes (b) 4 minutes (c) 6 minutes (d) 8 minutes (e) 10 minutes	149

## LIST OF ABBREVIATIONS

AAQG	-	Ambient Air Quality Guidelines
AAQS	-	Ambient Air Quality Standard
ADMS	-	Atmospheric Dispersion Modelling System
AECOPD	-	Acute Exacerbations Of Chronic Obstructive Pulmonary Disease
AGREE	-	Accidental Gas Release
AMR	-	AMR Environmental Pte. Ltd.
AMS	-	American Meteorological Society
CALINE	-	California Line Source Model
CALPUFF	-	California Puff Modelling System
CFD	-	Computational Fluid Dynamics
CTDMPLUS	-	Complex Terrain Dispersion Model
GIS	-	Geo Information System
GLC	-	Ground-Level Concentration
IAQ	-	Indoor Air Quality
IOP	-	Intensive Observational Periods
IMMDADS	-	Integrated Malaysian Meteorological Data Atmospheric Dispersion Software
ISC	-	Industrial Source Complex
JU2003	-	Joint Urban 2003 Field Measurement
EIA	-	Environmental Impact Assessment
EPA	-	Environmental Protection Agency
ESRI	-	Environmental Systems Research
GPU	-	Graphics Processing Unit
KAMI	-	Kualiti Alam Modularized Incinerator
LES	-	Large Eddy Simulation
LIDAR	-	Light Detection and Ranging
LPG	-	Liquefied Petroleum Gas
NAME	-	Numerical Atmospheric-dispersion Modelling Environment
NO <sub>x</sub>	-	Oxides of Nitrogen

O <sub>3</sub>	-	Ozone
PM <sub>10</sub>	-	Particulate Matter 10 Micrometer in Size
PM <sub>2.5</sub>	-	Particulate Matter 2.5 Micrometer in Size
RAM	-	Random Access Memory
RANS	-	Reynolds Averaged Navier-Stokes
RGB	-	Red Green Blue
RMG	-	Recommended Malaysian Guidelines
SAR	-	Synthetic-Aperture Radar
SF <sub>6</sub>	-	Sulfur Hexaflouride
SRTM	-	Shuttle Radar Topography Mission
TDMA	-	Tri-Diagonal Matrix Algorithm

## LIST OF SYMBOLS

$\beta$	-	Artificial Compressibility
$C$	-	Pollutant Concentration
$D$	-	Molecular Diffusivity
$H$	-	Height of Cube
$h_e$	-	Effective Stack Height
$h_s$	-	Stack Height
$h'_s$	-	Effective Stack Height
$k$	-	Karman Constant
$K_c$	-	Turbulent Diffusivities of Scalar Variables
$l_{mix}$	-	Mixing Length
$\mu$	-	Kinematic Viscosity
$n$	-	Normal to Boundary
$\rho$	-	Fluid/Air Density
$p$	-	Power Law Exponents
$P$	-	Deviation of Pressure
$Q$	-	Stack Volumetric Flow Rate
$S_c$	-	Source/Sink Term of Pollutants
$SF_6$	-	Sulphur Hexafluoride
$T_a$	-	Ambient Air Temperature
$T_s$	-	Stack Gas Temperature
$t$	-	Time
$\tau_{ij}$	-	Reynolds Stress Tensor
$\tau$	-	Artificial Time
$u$	-	Wind Velocity
$U_c$	-	Velocity Independent of Outlet Plane
$U_i$	-	ith Mean Velocity Component
$u_s$	-	Wind Velocity at Stack Height
$U_t$	-	Friction Velocity
$U, V, W$	-	Velocity in X, Y and Z Directions

# CHAPTER 1

## INTRODUCTION

### 1.1 Research Background

Air pollutant release from transportation and industries have been major threat to human health and wellness in rural and urban areas (Tian *et al.*, 2019). Air pollutants are the early origin of respiratory diseases (Kim *et al.*, 2018) that need to be constantly monitored to preserve air quality and environment. One of the methods to control air pollution is by regulating law to limit permissible amount of harmful gases into the atmosphere. In order to do so, air pollution dispersion simulation is needed to estimate the allowable release amount and assess the impact of unhealthy chemical releases to the surrounding ambient atmosphere.

In environmental town planning, air pollutant prediction and simulation in urban industrial park is important to identify critical areas where pollutant entrapments are taken place due to vehicle emissions, industrial release, agricultural waste and construction dusts. They are used by urban planners for long-term air pollution risk and health assessments, evacuation plan during accidents and assists in smart city design with good ventilation resulting in effective natural pollutant removal process. Besides, the analysis prevents failed urban design such as developing residential areas around polluted areas as well as evade late warnings of severe pollution levels that adversely affect health of citizen in the long run. In addition, detailed simulation can also be used to locate strategic station for air cleaning devices in urban areas.

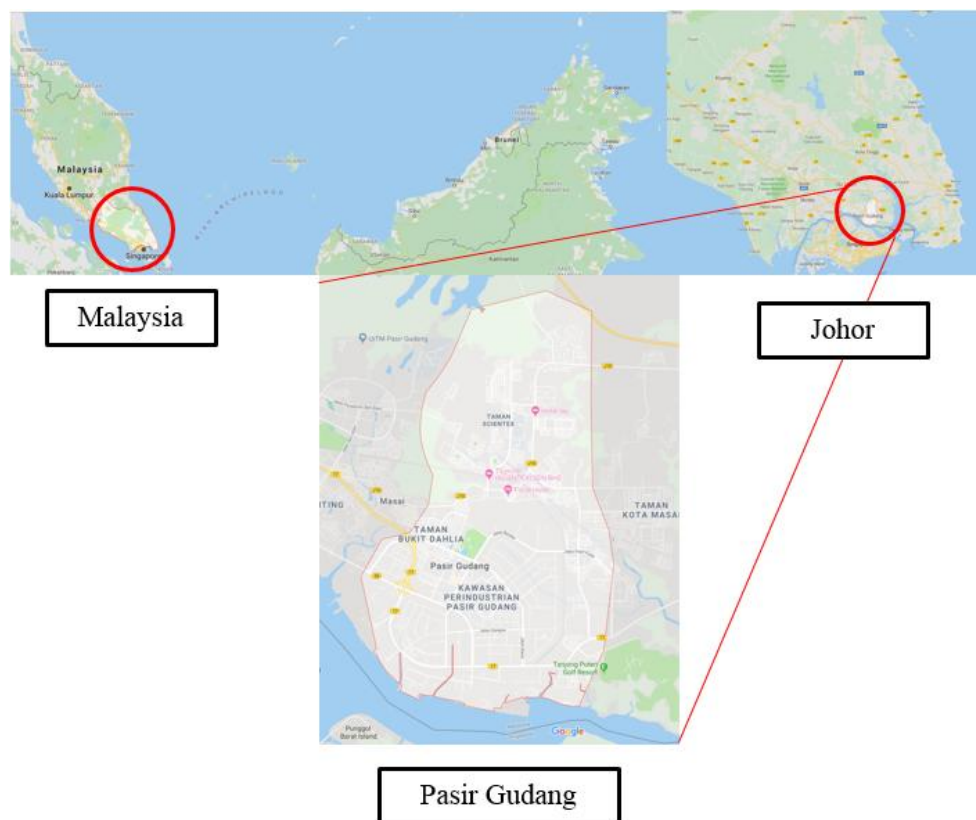
In practical use, air pollutants dispersion software are developed based on Gaussian Plume model. They are based on conical plume assumption in which the concentration across the plume cross-section has a Gaussian (normal) distribution. Those software are used to estimate the pollutant concentration on the ground around industrial stack such as the well-known U.S. Environmental Protection Agency (EPA)

Regulatory Model (AERMOD). This model is widely used for Environmental Impact Assessment (EIA) because it is sufficiently accurate, relatively simple to run with short computing time and low computer requirement. On average computer, for 50 x 50 number of grids with 200m distance between each grid (10 km x 10 km simulation area), those software usually take seconds to calculate 1 hour ground-level pollutant concentration (GLC) and approximately 15 to 40 minutes to calculate 1 year GLC. The Random Access Memory (RAM) used is relatively low compared to other advanced models since Gaussian Plume model can be run effectively with lower than 5000 number of grid points. However, Gaussian Plume model falls short in complex built environment due to flat terrain assumptions that were used during model development.

For complex urban structures, Computational Fluid Dynamics (CFD) models are better in handling three-dimensional (3D) air flow and pollutant dispersion within building configurations but it is less popular among environmental modellers due to high computing load required, complexity of the setup and long simulation times (Antonioni *et al.*, 2012). In practice, CFD models are only able to conduct simulation on approximately 1 km x 1 km x 1 km computational domain with lower than 10 m in grid size (approximately 1 million grid points). Though, it may take more than 1 hour to complete the calculation for steady flow and up to days and months for unsteady and transient flow. Moreover, the simulation times might increase significantly for larger CFD mesh (discrete grid points to solve air/fluid equations). In common, such simulations can take more than 1 GB of RAM usage on average computer. For these reasons, CFD analysis are generally not included in EIA analysis. Although air pollutant prediction and simulation has been studied extensively, no attempt has been made to analyse detailed wind distribution and pollutant dispersion process on high concentration zones in urban industrial park (network of stacks with nearby residential areas) predicted from conventional Gaussian Plume model.

In this study, both models are developed together in a single algorithm to complement their limitations. Due to poles apart models' structure, fundamental equations, coding architectures and massive programming effort to integrate both models in a single algorithm, there is no effort found in the literature on integrating both models as one. The primary advantage acquired by integrating both models in the

same algorithm is that it allows user to find the high concentration zones using Gaussian Plume model and further investigate pollutant dispersion process within the areas using CFD model. In this study, the code of both models are written from scratch to ensure unified programming structure in order to carry out the integration. The main difficulty of this study lies on figuring out coding implementation of collective governing equations and assuring accuracy, stability, efficiency and robustness of the algorithm. Integrated Gaussian and CFD model allow multiple scale air pollutant dispersion prediction commencing from regional/neighbourhood estimation of air pollution level using Gaussian Plume model in neighbourhood scale ( $10^4$  m in computational domain size) up to detailed building scale simulation ( $10^3$  m) using CFD model as shown in Figure 1.1 (residential area in Pasir Gudang) (Cui et al., 2016). Hence, ability of the present algorithm developed in this study ranging from conducting routine air pollution assessment for regional estimation of air pollution level to more detailed wind flow analysis within building structures in the urban industrial park.



(a)



Figure 1. 1 (a) Location of Pasir Gudang Industrial Park (b) Neighbourhood scale ( $10^4$  m or 10 km x 10 km using Gaussian Plume model) (c) Building scale ( $10^3$  m or 1 km x 1 km using CFD model) (Google Maps, 2019).

Applying CFD models on complex urban structures requires extra task to remodel the buildings. Although accuracy of CFD models are satisfactory in recent years, generating urban 3D building models for CFD solvers still require manual effort especially in highly populated areas with multiple building configurations. In commercial software such as the well-known ANSYS Fluent software, users need to manually model the buildings using third-party software such as SOLIDWORKS (Bock, 2015). In the present CFD model, a smart function to automatically generate CFD mesh consisting urban buildings using image processing of satellite image is developed. Even though modellers are able to obtain the building data from Geographic Information System (GIS) data centre, several limitations of GIS approach restrict the convenience of the process. Those constrains include digitizing accuracy, incomplete data for rural and remote areas, costly and time consuming to obtain the data, manual update that causes human error and require good understanding on software architecture to extract available information before data manipulation (Schmit *et al.*, 2006).

In contrast, this study proposes a more reliable and effective way to generate building geometries using satellite image for CFD simulation. This approach analyses building footprints information and estimates the height using shadow length to



produce urban geometries by extruding the footprints detected beforehand. Furthermore, this technique only requires Red Green Blue (RGB) satellite image (.jpg, .jpeg, .png) to process which is much easier to obtained, low in cost, faster data acquisition, good availability, low memory requirement, efficient building generation process, partially automated and suitable for repetitive building extraction for entire city mapping application. From our observation, upcoming technological utilization that are predicted to be impacting environmental modelling study is CFD and automatic building generation from satellite image. This study attempts to merge unique capabilities of both research areas to produce a smart algorithm that ease modelling in environmental studies.

In short, this study emphases on integrating Gaussian Plume algorithm alongside air flow and pollutant dispersion solver based on CFD model. Additional unique features on CFD model mesh generation for automatic building construction from satellite image is developed using building footprint detection and height estimation technique.

## **1.2 Problem Statement**

In standard practice, Gaussian Plume model (regional estimation of air pollution level in EIA analysis) and CFD models (detailed air flow and pollutant dispersion simulations) are used in different applications and purposes. Gaussian Plume models generally applied in predicting ground concentration from industrial stack release in EIA analysis, whereas CFD models are used to attain detailed wind flow and pollutant simulation in urban areas. By having both models in the same algorithm, town planners will be able to find areas in urban industrial park with severe pollutant concentration and further investigate those regions using CFD model. In order to achieve this, a new algorithm are developed from scratch as both models are developed separately due to dissimilar approaches, assumptions, fundamental principles, governing equations and parameters used in the models. The present algorithm is not restricted to provide regional estimation of air pollution level (as in commercial software packages), but also able to present detailed wind distribution,

pollutant dispersions and entrapment zones within respective areas that is crucial to monitor in the long run. Existing commercial atmospheric dispersion software is not capable to do so.

For air pollutant simulation across complex building structures, building data such as stored in GIS are hard to acquire, expensive in cost and usually less accurate for small cities and undeveloped areas. GIS data require manual update on regular basis to stay updated with newly developed areas and a large number of GIS personnel are needed to cover data for all cities. In addition, manual data update practice in GIS may cause human error as well as labour and time consuming. As for current CFD commercial software, users need to remodel buildings and obstacles which results in repetitive and tedious process for air pollutant mapping in town planning application. To our knowledge, an effective tool that is able to automatically produce CFD mesh from satellite image integrated with air pollutant simulation solver for urban planners is still unavailable. Besides, studies on CFD analysis on high concentration zones predicted by Gaussian Plume model within urban industrial park is lacking in the literature.

For that, present study integrates both Gaussian and CFD model with automated building generation algorithm from satellite image and apply the algorithm in high pollutant concentration zone in urban industrial park.

### **1.3 Research Objectives**

The objectives of the present study are:

- (a) To integrate urban building generator from satellite image, Gaussian Plume and CFD model.
- (b) To evaluate performance of the developed satellite image urban building generator, Gaussian Plume and CFD algorithms.

- (c) To analyse wind flow, air pollutant dispersion and critical zones at high ground-level concentration areas in urban industrial park.

#### **1.4 Significance of Study**

This study improves conventional air pollutant regulatory model by providing detailed analysis of wind flow and pollutant dispersion process at high concentration zones predicted by the Gaussian plume model. It enhances usage of CFD model alongside Gaussian Plume model for air pollutant modellers by providing relatively accurate and fast CFD solver using the least expensive turbulence model coupled with automated CFD urban mesh generator from satellite image. As a result, an integrated Gaussian and CFD solver is produced that is practical for regulatory use united with additional capabilities to get detailed simulation on highly concentrated areas. This study encourages the use of CFD model in EIA analysis to complement data provided by Gaussian Plume model.

#### **1.5 Scope of Study**

In this study, Gaussian Plume and CFD model are used. In the CFD model, Fractional Step Method is used as the steady-state wind flow solver, Prandtl Mixing Length model is used for turbulence calculation. In urban building generator algorithm, colour separation technique is used for building detection process whereas shadow length estimation is used for building footprint height extrusion.

This study focuses on simulation of non-reactive air pollutants (SO<sub>2</sub>, NO<sub>2</sub> and PM<sub>10</sub>) released from major industrial stacks in Pasir Gudang Industrial Park, Johor towards nearby residential areas. In the simulation, only industrial stacks emissions are considered without background pollutant concentration (previous day, month and year concentration) and external pollutant sources such as vehicular emissions and

construction sites are not taken into account. In this study, the air pollutants are assumed to be released towards a completely clean ambient atmosphere thus the ground pollutant concentration exerted to the nearby residential areas in Pasir Gudang are only contributed by respective industrial stacks emissions.

It is assumed that all buildings are on flat terrain without elevation (hills and mountains), no trees and bushes are considered and all buildings have flat rooftops in which building geometries are dependent on their footprint shapes for building extrusion process.

## REFERENCES

- Afzali A., Rashid M. (2014), Trends and prediction of air pollutants in Pasir Gudang Industrial Area, Johor, Malaysia. PhD Thesis. *Faculty of Chemical Engineering, Universiti Teknologi Malaysia*.
- Amini and Seyed, M.. (2018). “Modeling Dispersion of Emissions from Depressed Roadways.” *Atmospheric Environment* 186(July 2017): 189–97.
- Allegrini, J. (2018) ‘A wind tunnel study on three-dimensional buoyant flows in street canyons with different roof shapes and building lengths’, *Building and Environment*. Elsevier, 143(July), pp. 71–88.
- Allegrini, J. and Carmeliet, J. (2017) ‘Coupled CFD and building energy simulations for studying the impacts of building height topology and buoyancy on local urban microclimates’, *Urban Climate*. Elsevier B.V., 21, pp. 278–305.
- Alwis Pitts, D. A. and So, E. (2017) ‘Enhanced change detection index for disaster response, recovery assessment and monitoring of buildings and critical facilities—A case study for Muzaffarabad, Pakistan’, *International Journal of Applied Earth Observation and Geoinformation*. Elsevier, 63(July), pp. 167–177.
- Amorim, J. H., Rodrigues, V., Tavares, R., Valente, J. and Borrego, C. (2013) ‘CFD modelling of the aerodynamic effect of trees on urban air pollution dispersion’, *Science of The Total Environment*. Elsevier B.V., 461–462, pp. 541–551.
- Antonioni, G., Burkhart, S., Burman, J., Dejoan, A., Fusco, A., Gaasbeek, R., Gjesdal, T., Jäppinen, A., Riikonen, K., Morra, P., Parmhed, O. and Santiago, J. L. (2012) ‘Comparison of CFD and operational dispersion models in an urban-like environment’, *Atmospheric Environment*. Elsevier Ltd, 47, pp. 365–372.
- Azliyana, A., Talib, M. and Fariz, A. (2018) ‘Road traffic as an air pollutant contributor within an industrial park environment’, *Atmospheric Pollution Research*. Elsevier B.V., 9(4), pp. 680–687.
- Azrita, N., Mohd A., Mohd B., and Ahmad Z. (2015). “Bayesian Extreme for Modeling High PM 10 Concentration in Johor.” *Procedia Environmental Sciences* 30: 309–14.

- Bady, M. (2017) 'Evaluation of Gaussian Plume Model against CFD Simulations through the Estimation of CO and NO Concentrations in an Urban Area', *American Journal of Environmental Sciences*, 13(2), pp. 93–102.
- Bady, M., Kato, S., Ooka, R., Huang, H. and Jiang, T. (2006) 'Comparative study of concentrations and distributions of CO and NO in an urban area: Gaussian plume model and CFD analysis', *WIT Transactions on Ecology and the Environment*, 86, pp. 55–64.
- Beychok, Milton R. (2005). *Fundamentals Of Stack Gas Dispersion* (4th ed.). author-published. ISBN 0-9644588-0-2. (Chapter 8, page 124)
- Benedek, C., Shadaydeh, M., Kato, Z., Szirányi, T. and Zerubia, J. (2015) 'Multilayer Markov Random Field models for change detection in optical remote sensing images', *ISPRS Journal of Photogrammetry and Remote Sensing*. International Society for Photogrammetry and Remote Sensing, Inc. (ISPRS), 107, pp. 22–37.
- Beril, S. and Cem, U. (2008) 'Building Detection from Aerial Images using Invariant Color Features and Shadow Information', *Computer and Information Sciences, 2008. ISCIS '08. 2008 23rd International Symposium on Computer and Information Sciences*
- Bijad, E., Delavar, M. A. and Sedighi, K. (2016) 'CFD simulation of effects of dimension changes of buildings on pollution dispersion in the built environment', *Alexandria Engineering Journal*. Faculty of Engineering, Alexandria University, 55(4), pp. 3135–3144.
- Blocken, B., van der Hout, A., Dekker, J. and Weiler, O. (2015) 'CFD simulation of wind flow over natural complex terrain: Case study with validation by field measurements for Ria de Ferrol, Galicia, Spain', *Journal of Wind Engineering and Industrial Aerodynamics*. Elsevier, 147, pp. 43–57.
- Bock, S. (2015) 'New open-source ANSYS-SolidWorks-FLAC3D geometry conversion programs', *Journal of Sustainable Mining*. Elsevier Ltd, 14(3), pp. 124–132.
- Boppana, V. B. L., Wise, D. J., Ooi, C. C., Zhmayev, E. and Poh, H. J. (2019) 'CFD assessment on particulate matter filters performance in urban areas', *Sustainable Cities and Society*. Elsevier, 46(January), p. 101376.
- Brusca, S., Famoso, F., Lanzafame, R., Mauro, S., Garrano, A. M. C. and Monforte, P. (2016) 'Theoretical and Experimental Study of Gaussian Plume Model in

- Small Scale System', *Energy Procedia*. The Author(s), 101(September), pp. 58–65.
- Chen, B., Chen, Z., Deng, L., Duan, Y. and Zhou, J. (2016) 'Building change detection with RGB-D map generated from UAV images', *Neurocomputing*. Elsevier, 208, pp. 350–364.
- Chen, Y., Hong, T. and Piette, M. A. (2017) 'Automatic generation and simulation of urban building energy models based on city datasets for city-scale building retrofit analysis', *Applied Energy*. Elsevier, 205(April), pp. 323–335.
- Cheshmehzangi, A., Zhu, Y. and Li, B. (2017) 'Application of environmental performance analysis for urban design with Computational Fluid Dynamics (CFD) and EcoTect tools: The case of Cao Fei Dian eco-city, China', *International Journal of Sustainable Built Environment*, 6(1), pp. 102–112.
- Chew, L. W. and Norford, L. K. (2018) 'Pedestrian-level wind speed enhancement in urban street canyons with void decks', *Building and Environment*. Elsevier, 146(September), pp. 64–76.
- Choi, G. S., Lim, J. M., Sunny Lim, K. S., Kim, K. H. and Lee, J. H. (2018) 'Characteristics of regional scale atmospheric dispersion around Ki-Jang research reactor using the Lagrangian Gaussian puff dispersion model', *Nuclear Engineering and Technology*. Elsevier Ltd, 50(1), pp. 68–79.
- Chu, A. K. M., Kwok, R. C. W. and Yu, K. N. (2005) 'Study of pollution dispersion in urban areas using Computational Fluid Dynamics (CFD) and Geographic Information System (GIS)', *Environmental Modelling and Software*, 20(3), pp. 273–277.
- Cui, P.-Y., Li, Z. and Tao, W.-Q. (2016) 'Wind-tunnel measurements for thermal effects on the air flow and pollutant dispersion through different scale urban areas', *Building and Environment*. Elsevier Ltd, 97, pp. 137–151.
- Cui, P. Y., Li, Z. and Tao, W. Q. (2016) 'Buoyancy flows and pollutant dispersion through different scale urban areas: CFD simulations and wind-tunnel measurements', *Building and Environment*. Elsevier Ltd, 104, pp. 76–91.
- Department of Environment (DOE). (2019) . Pasir Gudang, Johor Air Pollution: Real-time Air Quality Index (AQI). available online : <http://aqicn.org/city/malaysia/johor/pasir-gudang/>
- Department of Environment (DOE). (2015) "Mitra Valley Sdn. Bhd. - Preliminary EIA for New Factory Construction". available online :

[https://ekas.doe.gov.my/ekas/eia/upload/Ex\\_Sum/201511151439500.Chapter%205PEIA%20Mitra%20Valley%20SB.pdf?s\\_JENIS\\_LAPORAN=PEIA&s\\_NEGERI=&s\\_TAHUN=2015&ViewMode=Print&ID\\_PROJEK=14765&ID=14765&jenis=PEIA](https://ekas.doe.gov.my/ekas/eia/upload/Ex_Sum/201511151439500.Chapter%205PEIA%20Mitra%20Valley%20SB.pdf?s_JENIS_LAPORAN=PEIA&s_NEGERI=&s_TAHUN=2015&ViewMode=Print&ID_PROJEK=14765&ID=14765&jenis=PEIA)

- Dhunny, A. Z., Lollchund, M. R. and Rughooputh, S. D. D. V. (2017) ‘Wind energy evaluation for a highly complex terrain using Computational Fluid Dynamics (CFD)’, *Renewable Energy*. Elsevier Ltd, 101, pp. 1–9.
- Dornaika, F., Moujahid, A., El Merabet, Y. and Ruichek, Y. (2016) ‘Building detection from orthophotos using a machine learning approach: An empirical study on image segmentation and descriptors’, *Expert Systems with Applications*. Elsevier Ltd, 58, pp. 130–142.
- Dominik B., 2017, <https://www.empa.ch/web/s503/urban-modelling>
- Dubois, C., Thiele, A. and Hinz, S. (2016) ‘Building detection and building parameter retrieval in InSAR phase images’, *ISPRS Journal of Photogrammetry and Remote Sensing*, 114, pp. 228–241.
- Efthimiou, G. C., Andronopoulos, S., Tavares, R. and Bartzis, J. G. (2017) ‘CFD-RANS prediction of the dispersion of a hazardous airborne material released during a real accident in an industrial environment’, *Journal of Loss Prevention in the Process Industries*. Elsevier Ltd, 46, pp. 23–36.
- Fallah-Shorshani, M., Shekarrizfard, M. and Hatzopoulou, M. (2017) ‘Integrating a street-canyon model with a regional Gaussian dispersion model for improved characterisation of near-road air pollution’, *Atmospheric Environment*. Elsevier Ltd, 153, pp. 21–31.
- Fang, W., Peng, C., Ming, T., de Richter, R. and Wang, Q. (2019) ‘Effect of moving vehicles on pollutant dispersion in street canyon by using dynamic mesh updating method’, *Journal of Wind Engineering and Industrial Aerodynamics*. Elsevier Ltd, 187(November 2018), pp. 15–25.
- Geng F., et al. (2019). “Dust Distribution and Control in a Coal Roadway Driven by an Air Curtain System : A Numerical Study.” *Process Safety and Environmental Protection* 121: 32–42.
- Giaiotti, D., Oshurok, D. and Skrynyk, O. (2018) ‘The Chernobyl nuclear accident<sup>137</sup>Cs cumulative depositions simulated by means of the CALMET/CALPUFF modelling system’, *Atmospheric Pollution Research*. Elsevier B.V., 9(3), pp. 502–512.



- Gowardhan, A. A., Pardyjak, E. R., Senocak, I. and Brown, M. J. (2011) ‘A CFD-based wind solver for an urban fast response transport and dispersion model’, *Environmental Fluid Mechanics*, 11(5), pp. 439–464.
- Grinias, I., Panagiotakis, C. and Tziritas, G. (2016) ‘MRF-based segmentation and unsupervised classification for building and road detection in peri-urban areas of high-resolution satellite images’, *ISPRS Journal of Photogrammetry and Remote Sensing*. International Society for Photogrammetry and Remote Sensing, Inc. (ISPRS), 122, pp. 145–166.
- Hasfazilat, A., Ahmad, S. Y. and Nor, A. R. (2015). "The Malaysia PM<sub>10</sub> Analysis using Extreme Value." *Journal of Engineering Science and Technology*. Vol. 10, No. 12, pp.1560-1574.
- Hashem, M., Sri, H., and Suriya, V. (2017). “AERMOD for Near-Road Pollutant Dispersion : Evaluation of Model Performance with Different Emission Source Representations and Low Wind Options.” *Transportation Research Part D* 57(October): 392–402.
- He, T., Wang, T. and Zhang, H. (2018) ‘The use of artificial compressibility to improve partitioned semi-implicit FSI coupling within the classical Chorin–Témam projection framework’, *Computers and Fluids*. Elsevier Ltd, 166, pp. 64–77.
- Hoinaski, L., Franco, D. and de Melo Lisboa, H. (2016) ‘Comparison of plume lateral dispersion coefficients schemes: Effect of averaging time’, *Atmospheric Pollution Research*. Elsevier Ltd, 7(1), pp. 134–141.
- Holnicki, P., Kałuszko, A. and Trapp, W. (2016) ‘An urban scale application and validation of the CALPUFF model’, *Atmospheric Pollution Research*, 7(3), pp. 393–402.
- Houda, S., Belarbi, R. and Zemmouri, N. (2017) ‘A CFD Comsol model for simulating complex urban flow’, *Energy Procedia*. Elsevier B.V., 139, pp. 373–378.
- Khan, J., Kakosimos, K., Raaschou-Nielsen, O., Brandt, J., Jensen, S. S., Ellermann, T. and Ketzel, M. (2019) ‘Development and performance evaluation of new AirGIS – A GIS based air pollution and human exposure modelling system’, *Atmospheric Environment*. Elsevier, 198(May 2018), pp. 102–121.
- Kim, D., Chen, Z., Zhou, L.-F. and Huang, S.-X. (2018) ‘Air pollutants and early origins of respiratory diseases’, *Chronic Diseases and Translational Medicine*. Elsevier Masson SAS, 4(2), pp. 75–94.
- Kranz, O., Lang, S. and Schoepfer, E. (2017) ‘2.5D change detection from satellite

- imagery to monitor small-scale mining activities in the Democratic Republic of the Congo', *International Journal of Applied Earth Observation and Geoinformation*. Elsevier, 61(May 2016), pp. 81–91.
- Kumar, P., Feiz, A.-A., Ngae, P., Singh, S. K. and Issartel, J.-P. (2015) 'CFD Simulation of Short-Range Plume Dispersion from a Point Release in an Urban like Environment', *Atmospheric Environment*. Elsevier Ltd.
- Kwak, K.-H., Baik, J.-J., Ryu, Y.-H. and Lee, S.-H. (2015) 'Urban air quality simulation in a high-rise building area using a CFD model coupled with mesoscale meteorological and chemistry-transport models', *Atmospheric Environment*. Elsevier Ltd, 100, pp. 167–177.
- Kwak, K. H. and Baik, J. J. (2012) 'A CFD modeling study of the impacts of NO<sub>x</sub> and VOC emissions on reactive pollutant dispersion in and above a street canyon', *Atmospheric Environment*. Elsevier Ltd, 46(x), pp. 71–80.
- Lateb, M., Meroney, R. N., Yataghene, M., Fellouah, H., Saleh, F. and Boufadel, M. C. (2016) 'On the use of numerical modelling for near-field pollutant dispersion in urban environments - A review', *Environmental Pollution*, 208, pp. 271–283.
- Li, Z., Xu, J., Ming, T., Peng, C., Huang, J. and Gong, T. (2017) 'Numerical Simulation on the Effect of Vehicle Movement on Pollutant Dispersion in Urban Street', *Procedia Engineering*. Elsevier B.V., 205, pp. 2303–2310.
- Liasis, G. and Stavrou, S. (2016) 'Satellite images analysis for shadow detection and building height estimation', *ISPRS Journal of Photogrammetry and Remote Sensing*. International Society for Photogrammetry and Remote Sensing, Inc. (ISPRS), 119, pp. 437–450.
- Liew, J., Latif, M. T. and Tangang, F. (2011) 'Factors in influencing the variations of PM<sub>10</sub> aerosol dust in Klang Valley, Malaysia during the summer', *Atmospheric Environment*. Elsevier Ltd, 45(26), pp. 4370–4378.
- Liu, Z., Xie, M., Tian, K. and Gao, P. (2017) 'GIS-based analysis of population exposure to PM<sub>2.5</sub> air pollution—A case study of Beijing', *Journal of Environmental Sciences*. Elsevier B.V., 59, pp. 48–53.
- Long, Z., Liu, S., Pan, W., Zhao, X., Cheng, X., Zhang, H. and Chen, Q. (2018) 'Influence of surrounding buildings on wind flow around a building predicted by CFD simulations', *Building and Environment*, 140(February), pp. 1–10.
- Manno-Kovacs, A. and Sziranyi, T. (2015) 'Orientation-selective building detection

- in aerial images', *ISPRS Journal of Photogrammetry and Remote Sensing*. International Society for Photogrammetry and Remote Sensing, Inc. (ISPRS), 108, pp. 94–112.
- Mo, Z. and Liu, C. H. (2018) 'Wind tunnel measurements of pollutant plume dispersion over hypothetical urban areas', *Building and Environment*. Elsevier, 132(February), pp. 357–366.
- Oyarzun, G., Borrell, R., Gorobets, A., Mantovani, F. and Oliva, A. (2018) 'Efficient CFD code implementation for the ARM-based Mont-Blanc architecture', *Future Generation Computer Systems*. Elsevier B.V., 79, pp. 786–796.
- Patnaik, G., Pullen, J., Boris, J. P., Iselin, J. and Young, T. (2004) 'A comparison of contaminant plume statistics from a Gaussian puff and urban CFD model for two large cities', *Atmospheric Environment*, 39(6), pp. 1049–1068.
- Peña, P. A., Hernández, J. A. and Toro, V. M. (2010) 'Computational evolutionary inverse lagrangian puff model', *Environmental Modelling and Software*. Elsevier Ltd, 25(12), pp. 1890–1893.
- Pontiggia, M., Landucci, G., Busini, V., Derudi, M., Alba, M., Scaioni, M., Bonvicini, S., Cozzani, V. and Rota, R. (2011) 'CFD model simulation of LPG dispersion in urban areas', *Atmospheric Environment*. Elsevier Ltd, 45(24), pp. 3913–3923.
- Qi, F., Zhai, J. Z. and Dang, G. (2016) 'Building height estimation using Google Earth', *Energy and Buildings*. Elsevier B.V., 118, pp. 123–132.
- Radhika, S., Tamura, Y. and Matsui, M. (2015) 'Cyclone damage detection on building structures from pre- and post-satellite images using wavelet based pattern recognition', *Journal of Wind Engineering and Industrial Aerodynamics*. Elsevier, 136, pp. 23–33.
- Ramm, A. G. (2019) 'Solution of the Navier–Stokes problem', *Applied Mathematics Letters*. Elsevier Ltd, 87, pp. 160–164.
- Rafiqul M. I. (2011). "Assessment Of Wind Energy Potential Mapping For Peninsular Malaysia", Masters Thesis, Faculty of Engineering, Universiti Malaya.
- Rosaida, N. et al. (2018). "Time Effects of High Particulate Events on the Critical Conversion Point of Ground-Level Ozone." *Atmospheric Environment* 187(June): 328–34.
- Rozana Z., Ismid, M., Said, M., Yang, J., Yahya, K. and Haron, Z. (2009) 'Indoor Environment Sustainability Of Residential - Industrial Housing in Malaysia',

21(1), pp. 98–109.

- Sabatino, S., Buccolieri, R., Pulvirenti, B. and Britter, R. (2007) ‘Simulations of pollutant dispersion within idealised urban-type geometries with CFD and integral models’, *Atmospheric Environment*, 41(37), pp. 8316–8329.
- Sagan, V., Pasken, R., Zarauz, J. and Krotkov, N. (2018) ‘SO<sub>2</sub> trajectories in a complex terrain environment using CALPUFF dispersion model, OMI and MODIS data’, *International Journal of Applied Earth Observation and Geoinformation*. Elsevier, 69(March), pp. 99–109.
- Sanchez, B., Santiago, J. L., Martilli, A., Martin, F., Borge, R., Quaassdorff, C. and de la Paz, D. (2017) ‘Modelling NOX concentrations through CFD-RANS in an urban hot-spot using high resolution traffic emissions and meteorology from a mesoscale model’, *Atmospheric Environment*. Elsevier Ltd, 163(X), pp. 155–165.
- Sáňka, O., Melymuk, L., Čupr, P., Dvorská, A. and Klánová, J. (2014) ‘Dispersion modeling of selected PAHs in urban air: A new approach combining dispersion model with GIS and passive air sampling’, *Atmospheric Environment*, 96, pp. 88–95.
- Schatzmann, M. and Leitl, B. (2011) ‘Issues with validation of urban flow and dispersion CFD models’, *Journal of Wind Engineering and Industrial Aerodynamics*. Elsevier, 99(4), pp. 169–186.
- Schmit, C., Rounsevell, M. D. A. and La Jeunesse, I. (2006) ‘The limitations of spatial land use data in environmental analysis’, *Environmental Science and Policy*, 9(2), pp. 174–188.
- Sha, C., Hou, J. and Cui, H. (2016) ‘A robust 2D Otsu’s thresholding method in image segmentation’, *Journal of Visual Communication and Image Representation*. Elsevier Inc., 41, pp. 339–351.
- Shirzadi, M., Naghashadegan, M. and A. Mirzaei, P. (2018) ‘Improving the CFD modelling of cross-ventilation in highly-packed urban areas’, *Sustainable Cities and Society*. Elsevier, 37(November 2017), pp. 451–465.
- Sirmaçek, B. and Ünsalan, C. (2008) ‘Building detection from aerial images using invariant color features and shadow information’, *2008 23rd International Symposium on Computer and Information Sciences, ISCIS 2008*.
- Smith, R. J. (1995) ‘A Gaussian model for estimating odour emissions from area sources’, *Mathematical and Computer Modelling*, 21(9), pp. 23–29.

- Soergel, U., Michaelsen, E., Thiele, A., Cadario, E. and Thoennesen, U. (2009) ‘Stereo analysis of high-resolution SAR images for building height estimation in cases of orthogonal aspect directions’, *ISPRS Journal of Photogrammetry and Remote Sensing*. Elsevier B.V., 64(5), pp. 490–500.
- Sumer, E. and Turker, M. (2013) ‘An adaptive fuzzy-genetic algorithm approach for building detection using high-resolution satellite images’, *Computers, Environment and Urban Systems*. Elsevier Ltd, 39, pp. 48–62.
- Sun, Y., Moshfeghi, Y. and Liu, Z. (2017) ‘Exploiting crowdsourced geographic information and GIS for assessment of air pollution exposure during active travel’, *Journal of Transport and Health*. Elsevier Ltd, 6(March), pp. 93–104.
- Szabo Aron (2016) 'Dissipative quantum transport simulations in two-dimensional semiconductor devices from first principles', PHD Thesis. Budapest University of Technology and Economics,
- Tahara, Y., Katsui, T. and Himeno, Y. (2011) ‘Computation of Ship Viscous Flow at Full Scale Reynolds Number’, *Journal of the Society of Naval Architects of Japan*, 2002(192), pp. 89–101.
- Tang, W., Foroutan, H., Monbureau, E. M., Heist, D. K., Brouwer, L. H. and Perry, S. G. (2018) ‘Enhancements to AERMOD’s building downwash algorithms based on wind-tunnel and Embedded-LES modeling’, *Atmospheric Environment*. Elsevier, 179 (February), pp. 321–330.
- Tartakovsky, D., Stern, E. and Broday, D. M. (2016) ‘Comparison of dry deposition estimates of AERMOD and CALPUFF from area sources in flat terrain’, *Atmospheric Environment*. Elsevier Ltd, 142, pp. 430–432.
- Tian, Y., Yao, X. and Chen, L. (2019) ‘Analysis of spatial and seasonal distributions of air pollutants by incorporating urban morphological characteristics’, *Computers, Environment and Urban Systems*. Elsevier, 75(November 2018), pp. 35–48.
- Toja-Silva, F., Chen, J., Hachinger, S. and Hase, F. (2017) ‘CFD simulation of CO<sub>2</sub> dispersion from urban thermal power plant: Analysis of turbulent Schmidt number and comparison with Gaussian plume model and measurements’, *Journal of Wind Engineering and Industrial Aerodynamics*. Elsevier Ltd, 169(March), pp. 177–193.
- Toja-Silva, F., Pregel-Hoderlein, C. and Chen, J. (2018a) ‘On the urban geometry generalization for CFD simulation of gas dispersion from chimneys:

- Comparison with Gaussian plume model’, *Journal of Wind Engineering and Industrial Aerodynamics*. Elsevier Ltd, 177(April), pp. 1–18.
- Toja-Silva, F., Pregel-Hoderlein, C. and Chen, J. (2018b) ‘On the urban geometry generalization for CFD simulation of gas dispersion from chimneys: Comparison with Gaussian plume model’, *Journal of Wind Engineering and Industrial Aerodynamics*. Elsevier Ltd, 177(December 2017), pp. 1–18.
- Tong, X., Lin, X., Feng, T., Xie, H., Liu, S., Hong, Z. and Chen, P. (2013) ‘Use of shadows for detection of earthquake-induced collapsed buildings in high-resolution satellite imagery’, *ISPRS Journal of Photogrammetry and Remote Sensing*. International Society for Photogrammetry and Remote Sensing, Inc. (ISPRS), 79, pp. 53–67.
- Toparlar, Y., Blocken, B., Maiheu, B. and van Heijst, G. J. F. (2017) ‘A review on the CFD analysis of urban microclimate’, *Renewable and Sustainable Energy Reviews*. Elsevier Ltd, 80(January), pp. 1613–1640.
- Ubaidullah S., Osman, K., Mohd Rashid, A. and Ammar Kusnin, N. H. (2015) ‘Integrated Malaysian Meteorological Data Atmospheric Dispersion Software (IMMDADS)’, *Jurnal Teknologi (Science & Engineering)*, 72, pp. 1–6.
- U.Ghia, K.N.Ghia and C.T.Shin (1982) ‘High-Re solutions for incompressible flow using the Navier-Stokes equations and a multigrid method’, *Journal of Computational Physics*, 48, pp. 387–411.
- U.S. Government Accountability Office (US GAO), 2017, available online at <https://www.nationalgeographic.org/encyclopedia/geographic-information-system-gis/>.
- Vranckx, S., Vos, P., Maiheu, B. and Janssen, S. (2015) ‘Impact of trees on pollutant dispersion in street canyons: A numerical study of the annual average effects in Antwerp, Belgium’, *Science of the Total Environment*. Elsevier B.V., 532, pp. 474–483.
- Wang, S., Zhong, Y. and Wang, E. (2019) ‘An integrated GIS platform architecture for spatiotemporal big data’, *Future Generation Computer Systems*. Elsevier B.V., 94, pp. 160–172.
- Wang, W., Xu, Y. and Ng, E. (2017) ‘Large-eddy simulations of pedestrian-level ventilation for assessing a satellite-based approach to urban geometry generation’, *Graphical Models*. Elsevier Inc., 95, pp. 29–41.
- Wang, W., Xu, Y., Ng, E. and Raasch, S. (2018) ‘Evaluation of satellite-derived

- building height extraction by CFD simulations: A case study of neighborhood-scale ventilation in Hong Kong', *Landscape and Urban Planning*. Elsevier, 170(September 2017), pp. 90–102.
- Wang, W., Ying, Y., Wu, Q., Zhang, H., Ma, D. and Xiao, W. (2015) 'A GIS-based spatial correlation analysis for ambient air pollution and AECOPD hospitalizations in Jinan, China', *Respiratory Medicine*. Elsevier Ltd, 109(3), pp. 372–378.
- Xiang, Y., Yu, B., Yuan, Q. and Sun, D. (2017) 'GPU Acceleration of CFD Algorithm: HSMAC and SIMPLE', *Procedia Computer Science*, 108, pp. 1982–1989.
- Xing, Y. and Brimblecombe, P. (2019) 'Role of vegetation in deposition and dispersion of air pollution in urban parks', *Atmospheric Environment*. Elsevier, 201(November 2018), pp. 73–83.
- Yeo, I. A., Yoon, S. H. and Yee, J. J. (2013) 'Development of an environment and energy Geographical Information System (E-GIS) construction model to support environmentally friendly urban planning', *Applied Energy*, 104, pp. 723–739.
- Zhang, Y. (1999) 'Optimisation of building detection in satellite images by combining multispectral classification and texture filtering', *ISPRS Journal of Photogrammetry and Remote Sensing*, 54(1), pp. 50–60.

## LIST OF PUBLICATIONS

S. Ubaidullah, K. Osman, M. R. Ammar, A. K. Noor Hafizah, “Evaluation Of Integrated Malaysian Meteorological Data Atmospheric Dispersion Software (IMMDADS)”, Published In Advanced Science Letters, Vol. 23 No. 5, Pp. 4399-4404(6) (2017)

Ubaidullah Selamat, Kahar Osman, Arul Hisham A. Rahim, “Heat and Flow Analysis of a Chilled Water Storage System using Computational Fluid Dynamics”, accepted in Journal of Advanced Research in Fluid Mechanics and Thermal Sciences.